Immunology
The Journal of cells, molecules, systems and technologies

British Society for immunology

IMMUNOLOGY ORIGINAL ARTICLE

Steric recognition of T-cell receptor contact residues is required to map mutant epitopes by immunoinformatical programmes

Shiou-Chih Hsu,[1] Chih-Peng Chang,[2] Chao-Yuan Tsai,[2] Shih-Hung Hsieh,[3] Betty A. Wu-Hsieh,[3] Yu-Shu Lo[4] and Jinn-Moon Yang[4]

[1]*Vaccine Research and Development Centre, National Health Research Institute, Miaoli County, Taiwan,* [2]*Microbiology and Immunology, NCKU, Tainan, Taiwan,* [3]*Immunology, NTU, Taipei, Taiwan, and* [4]*Biological Science and Technology, NCTU, Hsinchu, Taiwan*

doi:10.1111/j.1365-2567.2011.03542.x
Received 24 August 2011; revised 22 November 2011; accepted 23 November 2011.
Correspondence: Dr Shiou-Chih Hsu, Vaccine Research and Development Centre, National Health Research Institutes, R1-7031 Office, 35 Keyan Road, Zhunan, Miaoli County 350, Taiwan.

Summary

MHC class I-restricted CD8 T-lymphocyte epitopes comprise anchor motifs, T-cell receptor (TCR) contact residues and the peptide backbone. Serial variant epitopes with substitution of amino acids at either anchor motifs or TCR contact residues have been synthesized for specific interferon-γ responses to clarify the TCR recognition mechanism as well as to assess the epitope prediction capacity of immunoinformatical programmes. CD8 T lymphocytes recognise the steric configuration of functional groups at the TCR contact side chain with a parallel observation that peptide backbones of various epitopes adapt to the conserved conformation upon binding to the same MHC class I molecule. Variant epitopes with amino acid substitutions at the TCR contact site are not recognised by specific CD8 T lymphocytes without compromising their binding capacity to MHC class I molecules, which demonstrates two discrete antigen presentation events for the binding of peptides to MHC class I molecules and for TCR recognition. The predicted outcome of immunoinformatical programmes is not consistent with the results of epitope identification by laboratory experiments in the absence of information on the interaction with TCR contact residues. Immunoinformatical programmes based on the binding affinity to MHC class I molecules are not sufficient for the accurate prediction of CD8 T-lymphocyte epitopes. The predictive capacity is further improved to distinguish mutant epitopes from the non-mutated epitopes if the peptide–TCR interface is integrated into the computing simulation programme.

Keywords: CD8/cytotoxic T cells; major histocompatibility complexes/HLA; T-cell receptor; T cells; vaccines

Introduction

Specific CD8 T-lymphocyte responses are important in recovery from respiratory syncytial virus (RSV) infection[1–3] as well as for protection against heterotypic influenza viruses.[4–6] Formalin-inactivated vaccines are not formulated to prime for MHC class I-restricted CD8 T-lymphocyte responses.[7,8] Similar to inactivated vaccines, purified protein antigens are not effective at activation of CD8 T-lymphocyte responses despite the presence of adjuvants.[9–11] Complications of adjuvant formulations often enhance one arm of immune effectors but inhibit another.[11]

Immunisation with synthetic peptide vaccines is a promising approach to protection against viral infections via the induction of specific CD8 T-lymphocyte responses.[12–15] Hence, identification of protective epitopes is a priority in the development of synthetic peptide vaccines.[12,16] In particular, the identification of immunodominant epitopes is indispensable for the prevention of mutable viruses[16,17] even if the non-immunodominant epitope provides partial protection against influenza virus infection.[14]

CD8 T lymphocytes recognise peptides presented by MHC class I molecules.[18] MHC class I-restricted peptides contain 8–12 amino acids.[19–26] Since procedures of peptide–

Abbreviations: ELISPOT, enzyme-linked immunospot; H1N1 A/WSN/33, one subtype of influenza viruses; IFN, interferon; MACS, magnetic cell separation; MFI, mean fluorescence intensity; MHC, major histocompatibility complexes; RSV, respiratory syncytial virus; TCR, T-cell receptor.

MHC class I binding experiments are becoming complicated, many immunoinformatical programmes have been developed to predict epitopes, even prior to any laboratory experiments.[19,27–32] Bioinformatical programmes can be classified into sequence-based,[19,27,33,34] integrative[29] and structure-based approaches,[35,36] which are not integrated with the recognition interface between peptide–MHC class I molecules and T-cell receptors (TCR) for immunological purposes. An increasing number of MHC class I–peptide–TCR structures were analysed by X-ray diffraction, so the structure-based simulation approach has been exploited in this research to provide insights in the structure with the aim of developing an immunoinformatical programme for a further demonstration of the recognition mechanism found in our laboratory experiments. For the research described here, we attempt to clarify the impact of TCR contact residues on the TCR recognition mechanism as well as on the prediction accuracy on CD8 T-lymphocyte epitopes from protein sequences by immunoinformatical programmes for the rational design of T-lymphocyte epitope vaccines.

Materials and methods

Peptide synthesis

Peptides were synthesized with Fmoc chemistry (Iris Biotech GmbH Co., Germany & Mission Biotech Co., Taiwan). Synthesized peptides were purified with HPLC and confirmed with mass spectrometry for 95% purity. Variant peptides were synthesized with amino acid substitutions at either anchor motifs (P2 or P9) or TCR contact sites (P6 or P8). Peptide sequences are presented in Table 1.

Cells and virus culture

The lack of TAP function enables RMA-S cells to be used as a measure of the binding of peptides to different MHC class I alleles on the cell surface.[37] RMA-S-K^d cells are H-$2K^d$-transfected TAP function-deficient lymphoma cells.[38] RMA, RMA-S, and RMA-S-K^d cells proliferated in RPMI-1640/1 × medium for peptide–MHC class I binding experiments (Gibco Co. & Hyclone Co.). Transfected TAP-mutant cells are kind gifts from National Institute of Allergy and Infectious Diseases, National Institutes of Health (NIH), USA.

The RSV was multiplied in HEp-2 cells that were grown with minimum essential medium/1 × (Gibco Co. & Hyclone Co.). Virus was further titrated with plaque assay in HEp-2 cells. The RSV was obtained from the American Type Culture Collection. As presented in the Supplementary material, Fig. S1, influenza A/WSN/33 virus[39] was multiplied in MDCK cells cultivated with Dulbecco's modified Eagle's minimal essential medium/1 × (Gibco Co. & Hyclone Co.). The quantification of the H1N1 A/WSN/33 virus was performed with a plaque assay in MDCK cells. Influenza A/WSN/33 virus was provided by Professor Betty A. Wu-Hsieh, which was purchased from the Department of Medical Biotechnology and Laboratory Science, Chang Kung University. The virus was cultivated in the USA. Influenza A/WSN/33 virus originated from the UK.[39]

Binding experiments of epitopes to MHC class I molecules

The TAP function-deficient cells can distinguish peptides with higher affinity to MHC class I molecules from those

Table 1. Variant peptides with substitution at anchor motifs or the T-cell receptor contact site

Peptide designation	P1	P2	P3	P4	P5	P6	P7	P8	P9	MHC	Sources	Peptide type
M2:82–90 (M9)	S	Y	I	G	S	I	N	N	I	H-$2K^d$	[1]M2–1	Original
SG	S	G	I	G	S	I	N	N	I	H-$2K^d$	M2–1	Anchor variant
SC	S	C	I	G	S	I	N	N	I	H-$2K^d$	M2–1	Anchor variant
SH	S	H	I	G	S	I	N	N	I	H-$2K^d$	M2–1	Anchor variant
SF	S	F	I	G	S	I	N	N	I	H-$2K^d$	M2–1	Anchor variant
SW	S	W	I	G	S	I	N	N	I	H-$2K^d$	M2–1	Anchor variant
NG	S	Y	I	G	S	I	N	G	I	H-$2K^d$	M2–1	TCR variant
ND	S	Y	I	G	S	I	N	D	I	H-$2K^d$	M2–1	TCR variant
NQ	S	Y	I	G	S	I	N	Q	I	H-$2K^d$	M2–1	TCR variant
NE	S	Y	I	G	S	I	N	E	I	H-$2K^d$	M2–1	TCR variant
NNG	S	Y	I	G	S	I	N	N	G	H-$2K^d$	M2–1	Anchor variant
NS2:114–121	R	T	F	S	F	Q	L	I	[2]X	H-$2K^b$	[3]NS2	Original
GQ	R	T	F	S	G	Q	L	I	X	H-$2K^b$	NS2	Anchor variant
FG	R	T	F	S	F	G	L	I	X	H-$2K^b$	NS2	TCR variant

[1]M2–1 is derived from the original reading frame of respiratory syncytial virus matrix 2 protein.

[2]NS2:114–121 contains only eight amino acids.

[3]NS2 is the non-structural protein 2 derived from influenza A/WSN/33 virus.

with lower affinity. To detect the binding to different MHC class I alleles by variant peptides (Table 1) that are derived either from RSV or from influenza A virus, RMA-S and RMA-S-K^d cells were incubated with 10 μM of synthetic peptides at 37° following inducible expression of H-2 molecules at lower temperature.

Comparison of peptide–MHC class I binding affinity between distinct variant peptides and the original M2:82–90, RMA-S-K^d cells were incubated with a serial dilution of M2:82–90 as well as with each variant peptide derived from M2:82–90 (Table 1) for measurement of the binding capacity of these peptides to H-$2K^d$ molecules. The expression level of MHC class I molecules is presented as a shifted percentage of mean fluorescence intensity (MFI). The equation for calculation of the shifted percentage of MFI is as follows:

Shifted percentage of MFI = $[(MFI_{variant} - MFI_{control})/(MFI_{original} - MFI_{control}) - 1] \times 100\%$

where $MFI_{original}$ is the MFI of the original epitope, $MFI_{variant}$ is the MFI of variant epitopes and $MFI_{control}$ is the MFI of the peptide without binding.

Animal experiments of virus infection

BALB/c mice were infected with 10^5–10^6 plaque-forming units of RSV via the intranasal route. Two to three weeks following infection, spleen mononuclear cells from infected BALB/c mice were isolated to be re-stimulated *in vitro* with synthetic peptides derived from the RSV M2–1 protein sequence overnight for analysis of specific interferon-γ (IFN-γ) responses by the ELISPOT assay[13] (BD Biosciences Co.). BALB/c mice were provided by the National Laboratory Animal Centre in Taiwan.

C57BL/6 mice were injected with 10^3–10^5 plaque-forming units of influenza A/WSN/33 virus via intra-tracheal or intravenous route.[40] Two to three weeks following infection, spleen mononuclear cells were isolated for *in vitro* re-stimulation with synthetic peptides from the NS2 protein sequence of H1N1 A/WSN/33 virus for analysis of specific IFN-γ responses by the ELISPOT assay. C57BL/6 mice were purchased from Jackson Laboratory (Bar Harbor, ME) and bred at the Laboratory Animal Centre, National Taiwan University College of Medicine.

The use of animals for experiments has been reviewed and approved by the institutional committee at the animal facility of the National Health Research Institute in Taiwan.

ELISPOT assays and isolation of immunocytes with MACS sets

Spleen mononuclear cells from either RSV-infected BALB/c mice or H1N1 A/WSN/33 virus-infected C57BL/6 mice were re-stimulated *in vitro* with synthetic peptides in ELISPOT plates pre-coated with anti-IFN-γ antibodies for the detection of IFN-γ-producing cells. Following *in vitro* re-stimulation, specific IFN-γ spots were revealed with horseradish peroxidase-conjugated anti-IFN-γ antibodies and substrates.

CD8 T lymphocytes were further purified from mononuclear cells of RSV-infected BALB/c mice with MACS sets (Miltenyi Biotech Co., Germany) to be re-stimulated *in vitro* with peptide-pulsed antigen-presenting cells overnight for analysis by ELISPOT assays.[41]

Immunisation of BALB/c mice with variant epitopes for induction of specific CD8 T-lymphocyte responses

Subsequent to second or third subcutaneous immunisation with a variety of synthetic peptides emulsified in Freund's adjuvants, spleen mononuclear cells were isolated from BALB/c mice to be re-stimulated *in vitro* with the immunised peptide or others for analysis of specific IFN-γ responses by the ELISPOT assay (Table 1). BALB/c mice were supplied by the animal facility at the College of Medicine, National Cheng Kung University in Taiwan.

The prediction of CD8 T-lymphocyte epitopes by immunoinformatical programmes

Immunoinformatical programmes for epitope prediction involve the integration of various analysis domains for peptide–protein interaction.[19,27–32] The complete amino acid sequences of the RSV M2–1 and H1N1 A/WSN/33 virus NS2 proteins were retrieved from database websites of the National Centre for Biotechnology Information (NCBI; Bethesda, MD). Original sequences or sequences with substituted amino acids of the RSV M2–1 and H1N1 A/WSN/33 virus NS2 proteins at anchor motifs or the TCR contact site were inputted into computer servers of immunoinformatics, MHC BN Blast Search, Propred I, SVMHC, SYFPEITHI, NIH prediction server, CTLPred, Epijen' and BioXGEM for programme analysis to predict MHC class I-restricted CD8 T-lymphocyte epitopes.

Analysis of important amino acid for epitope prediction by bioinformatical programmes: scoring function and matrices

Inferred from X-ray diffracted crystal structures, several interaction forces are involved between the two interfaces of MHC–peptide–TCR complexes. The van der Waals force, hydrogen bond and electrostatic force of interaction interfaces were incorporated as separate domains in the prediction programme.[24] As significant variations of the peptide–TCR interface are inconsistent with the conserved side of the peptide–MHC, template similarity of bound peptides has been simulated with current MHC–peptide–TCR structures of the same MHC class I molecule to map mutant epitopes of high priority from other viral proteins.

We have proposed a template-based scoring function to determine the reliability of protein–protein interactions[36] and to identify template-based homologous protein complexes[42] derived from a structural complex. To measure the protein–peptide interaction score, the scoring function is defined as:

$$E_{\text{tot}} = E_{\text{vdw}} + E_{\text{SF}} + E_{\text{sim}} + wE_{\text{cons}}$$

in which E_{vdw} is the interacting van der Waals force; and E_{SF} are special bonds, for instance the hydrogen bond, electrostatic forces and the disulphide bond. E_{sim} is the similarity score of template interfaces, whereas E_{cons} is the couple-conserved amino acid score. W constant has been set to 3, based on our previous research on protein–protein interactions.

Results

Epitope prediction by anchor motifs

To some extent, anchor motifs have been successful in the prediction of CD8 T-lymphocyte epitopes.[19,43,44] The substitution of anchor motifs at P2 tyrosine (Y) or at P9 isoleucine (I) with glycine (G) abolished the binding of variant peptides, such as SG, to H-2K^{d} molecules (Table 1, Fig. 1a and Supplementary material, Fig. S2). The replacement of the anchor motif P5 phenylalanine (F) with glycine (G) blocked the binding of the variant peptide GQ to H-2K^{b} molecules (Table 1; Fig. 1b). These results have demonstrated the decisive role of anchor motifs in the binding of epitopes to MHC class I molecules. In contrast to this observation, previous studies have shown that many immunogenic and protective epitopes do not contain known anchor motifs.[22,45,46] In our experimental systems, exclusive of glycine (G), any substitution of known anchor motifs that reduced the binding of peptides to MHC class I molecules was still recognised by virus-specific CD8 T lymphocytes for fewer IFN-γ responses, for instance histidine (H) or cysteine (C) (Table 1; Figs 1c and 2a). These observations have indicated the limitation of anchor motifs to sort all potential epitopes with less binding affinity to MHC class I molecules.[22]

Epitope prediction by peptide binding affinity to MHC class I molecules

The substitution of the anchor motif P2 (Y) with phenylalanine (F) did not affect the binding affinity of SF to H-2K^{d} molecules, which was comparable to M2:82–90 (Table 1; Fig. 1c). The placement of cysteine (C), histidine (H) or tryptophan (W) at the P2 anchor motif reduced the binding affinity of variant peptides to H-2K^{d}

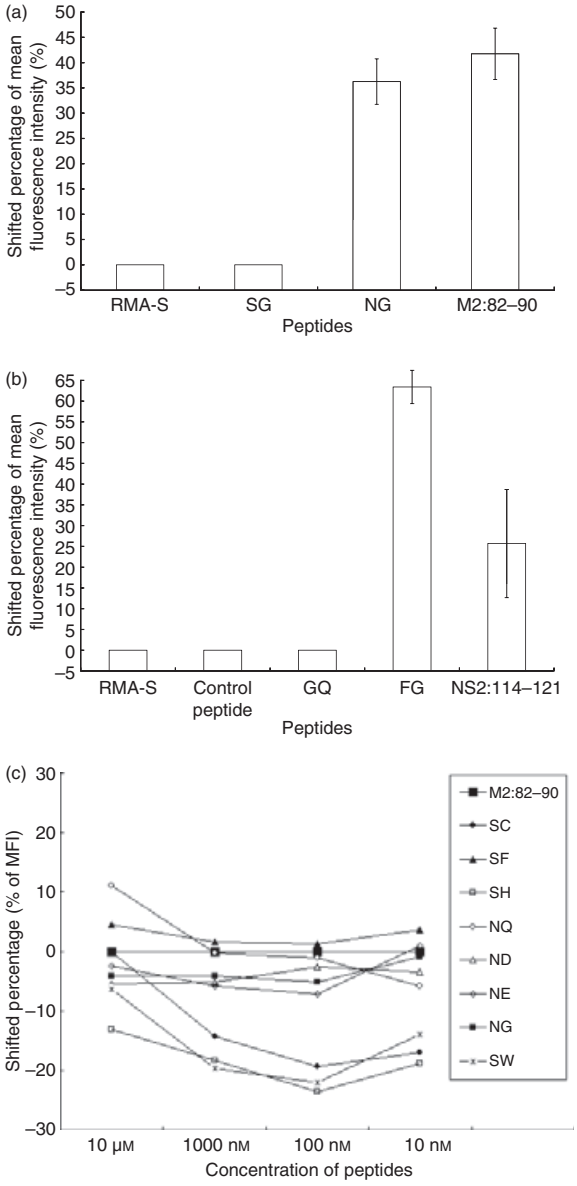

Figure 1. Expression of MHC class I molecules on TAP function-deficient cells pulsed with either variant epitopes or the original one. To compare the expression level of MHC class I molecules bound with a variety of peptides, RMA-S-K^{d} cells were incubated with 10 μM synthetic peptides: SG, NG and M2:82–90 (Fig. 1a). RMA-S cells were incubated with 10 μM synthetic peptides, such as NS2:114–121, GQ and FG (Fig. 1b). To determine the binding affinity of variant peptides, RMA-S-K^{d} cells were incubated in the presence of a serial dilution of each synthetic peptide: M2:82–90 (M9), SC, SF, SH, NG, NQ, NE, and SW (Table 1). Expression results of RMA-S-K^{d} cells bound with variant peptides were compared with those pulsed with M2:82–90 (Fig. 1c). After incubation with peptides, TAP function-deficient cells were stained with anti-H-2 IgG and FITC-labelled anti-IgG antibodies for flow cytometric analysis. The data of the binding of variant peptides to MHC class I molecules is presented as a shifted percentage of mean fluorescence intensity (MFI). The data in this figure have been reproduced in three independent experiments.

molecules, resembling SC, SH and SW (Table 1; Fig. 1c and Supplementary material, Fig. S3). Side chains of anchor motifs have a significant impact on the binding affinity of epitopes to MHC class I molecules. In contrast to the positive correlation between MHC class I binding affinity and epitope predictability, in recent years many epitopes with lower binding affinity to MHC class I molecules and subdominant epitopes have been identified as protective.[14,47,48] Variant peptides with substitutions at the TCR contact site were not recognised by specific CD8 T lymphocytes despite retaining the same extent of binding affinity as M2:82–90 (Table 1; Figs 1c, 2a, 3b and Supplementary material, Fig. S3). These results have illustrated the restriction of peptide–MHC binding affinity to map specific T-lymphocyte epitopes.

The relevance of TCR contact residues for CD8 T lymphocyte recognition

The recognition of variant peptide–MHC class I complexes by virus-specific CD8 T lymphocytes was analysed with ELISPOT assays for the detection of specific IFN-γ responses either from RSV-infected BALB/c mice or from H1N1 A/WSN/33 virus-infected C57BL/6 mice. The results confirmed that IFN-γ responses were from purified specific CD8 T lymphocytes (Fig. 2a). The experimental result of distinguishable specific IFN-γ responses is statistically significant between variant peptide-activated and the original peptide-activated CD8 T lymphocytes *in vitro* from RSV-infected BALB/c mice (Fig. 2a; $P < 0{\cdot}05$). Substitutions of asparagine (N) at TCR contact P8 site have

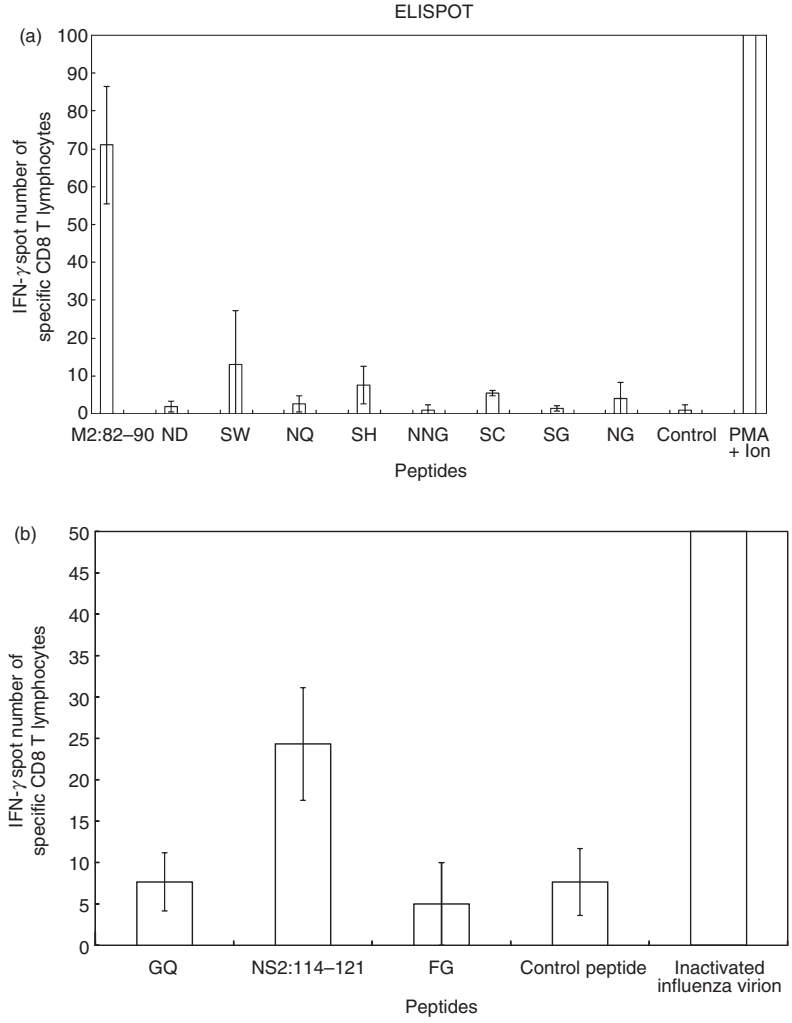

Figure 2. Specific interferon-γ (IFN-γ) responses of CD8 T lymphocytes from virus-infected murine cells re-stimulated with either variant epitopes or the original one. IFN-γ responses of CD8 T lymphocytes from respiratory syncytial virus (RSV) -infected BALB/c mice were re-stimulated *in vitro* with antigen-presenting cells pulsed with 1000 nM of each synthetic peptide: M2:82–90 (M9), SC, SH, ND, NG, SG, NNG, NQ, or SW (Fig. 2a). CD8 T-lymphocyte-mediated IFN-γ responses from H1N1 A/WSN/33 influenza virus-infected C57BL/6 mice were re-stimulated *in vitro* with synthetic peptides: NS2:114–121, GQ and FG (Fig. 2b). Specific IFN-γ responses were analysed with ELISPOT assays. PMA/ionomycin (PMA/Io) and inactivated influenza virions were included as a positive control for either specific CD8 T lymphocytes or mononuclear cells.

fully obstructed the recognition of variant peptide–MHC class I complexes by RSV-specific CD8 T lymphocytes regardless of diverse amino acids, for instance the analogous side chain of glutamine (N→Q) or heterologous side chains of aspartic acid and glycine (N→D or N→G) (Table 1; Fig. 2a). These substitutions of amino acids at the P8 site have not compromised their binding capacity to H-2K^d molecules with intact anchor motifs like the original (Table 1; Fig. 1c). In comparison with asparagine (N), there is only one extra functional group (-CH_2-) present at the side chain structure of glutamine (Q) or one distinctive functional group (-OH) at the structure of aspartic acid (D). The replacement of glutamine (Q) at the TCR contact P6 site with glycine (Q→G) has also impeded the recognition of variant peptide–MHC class I complexes by influenza A/WSN/33 virus-specific CD8 T lymphocytes (Table 1; Fig. 2b) without reducing the binding capacity to H-2K^b molecules (Fig. 1b).

BALB/c mice were immunised with variant peptides as well as the original for induction of peptide-specific IFN-γ responses. M2:82–90-specific CD8 T lymphocytes did not respond to a variant peptide NG for IFN-γ responses (Table 1; Fig. 3a,b). NG-specific CD8 T lymphocyte responses did not recognise M2:82–90 at level comparable to the immunised NG peptide (Fig. 3a,c). Variant peptide immunisation has demonstrated that TCR contact residues are important elements to affect the specificity of CD8 T-lymphocyte responses (Fig. 3).

Inaccurate epitope prediction by current immunoinformatical programmes

The full-length amino acid sequences of RSV M2–1 protein with either the original H-2K^d-restricted CD8 T-lymphocyte epitope or its variant epitopes were inputted into different available programmes for epitope prediction. The analysed data are presented in Table 2. According to the predicted range encompassing the original immunodominant epitope by discrete immunoinformatical servers, the top 10% of listed peptides are considered to be specific CD8 T-lymphocyte epitopes (Tables 2 and 3). As expected, M2:82–90 derived from the M2–1 protein with original amino acid sequences topped the predicted list of epitopes by programmes. Variant peptides with substituted amino acids at anchor motifs, apart from glycine (G), did not rank as high as M2:82–90 but still reached the top 5% of listed predicted epitopes from M2–1 protein with substituted amino acid sequences on several prediction servers (Tables 1 and 2). Certain servers ruled out a number of variant peptides with substituted amino acids at anchor motifs as MHC class I-restricted epitopes (Table 2). Variant peptides with substituted amino acids at anchor motifs, except for glycine, in this research should be ranked as epitopes of the prediction outcome, but often are not (Table 1; Fig. 2). The variant peptides with substituted TCR contact residues were still at the top of the predicted list of all servers as epitopes, the same as the original one, which is inconsistent with the experimental results for epitope identification (Tables 1 and 2; Figs 1 and 2).

The same analysed results were obtained for the majority of servers to predict the original H-2K^b-restricted CD8 T-lymphocyte epitope, NS2:114–121, derived from NS2 protein of H1N1 A/WSN/33 virus and its variant epitopes, GQ and FG, until the most recent programme BIOXGEM, which was integrated with interaction interfaces of the peptide–TCR, had been established (Tables 1 and 3; Figs 1 and 2). FG variant peptide with the substituted TCR contact residue was not predicted to be the specific CD8 T-lymphocyte epitope by BIOXGEM as indicated in the experimental result for epitope identification (Table 3; Fig. 2b).

Structural and biochemical features of important amino acids for epitope prediction

To evaluate the accuracy of scoring function on H2-K^b–peptide–TCR interactions, we simulate all H2-K^b–peptide–TCR crystal complexes as templates for epitope prediction. The experimental data for most of MHC-restricted peptides were collected from the IEDB database. Fifty-eight peptides have positive results whereas 66 peptides have negative results from both the MHC and TCR experimental records. We regard these peptides as standard positive and negative experimental sets for analysis to predict relevant CD8 T-lymphocyte epitopes. Each defined term of scoring functions was analysed with the receiver operating characteristics curve (Fig. 5a). The scoring function integrates the interface of binding forces ($E_{vdw} + E_{SF}$), amino acid conservation (E_{cons}) and template similarity (E_{sim}). The E_{cons} and E_{sim} have similar trends in their receiver operating characteristics curve, which is better than the dissimilar one for $E_{vdw} + E_{SF}$. These results reveal that the conserved amino acid position and the similarity between template and candidate proteins are perhaps more constant than binding forces, in particular for the peptide–MHC interface (Fig. 5a). The scoring function has the more constant prediction rate on the binding of peptides to MHC class I molecules than that to the TCR interface alone as far as the difference of analysis curves is concerned (Fig. 5b). Thus, to consider the template of MHC–peptide–TCR complexes as the whole structure with more than one interface, template similarity and binding forces are able to restore the predictability of scoring function without limitation from the biased number of conserved amino acid positions for MHC–peptide–TCR complexes (Table 3; Fig. 6).

While we put the scoring function into the operation of protein–peptide interactions such as MHC–peptide and peptide–TCR interfaces, the characteristics of pep-

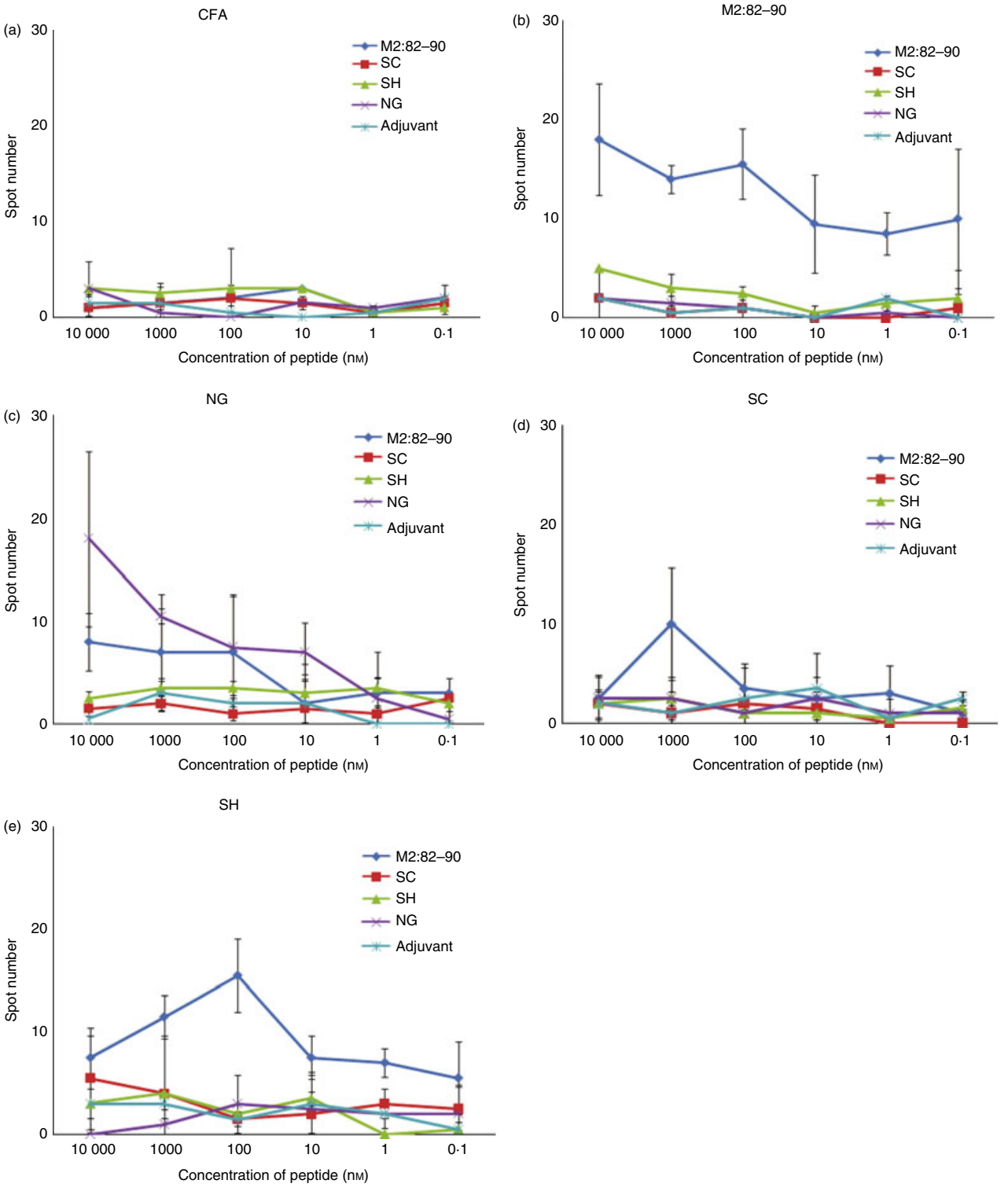

Figure 3. Specific CD8 T-lymphocyte-mediated interferon-γ (IFN-γ) responses from epitope-immunised BALB/c mice. Spleen mononuclear cells from BALB/c mice were re-stimulated *in vitro* with each immunised synthetic peptide following immunisation with adjuvants (Fig. 3a), M2:82–90 (Fig. 3b), NG (Fig. 3c), SC (Fig. 3d) or SH (Fig. 3e) peptides that was formulated in Freund's adjuvants (Table 1). Specific IFN-γ responses were analysed by ELISPOT assays.

Table 2.

Amino acids of the anchor motif P2	Prediction results of immunoinformatics servers	Recognised by H-2K^d-restricted respiratory syncytial virus-specific CD8 T lymphocytes
The original peptide M2:82–90: Tyrosine	MHC BN Blast search: + Propred I: + SVMHC: + SYFPEITHI: + NIH prediction server: + CTLPred: + Epijen: +	+
The variant peptide SC: Cysteine	MHC BN Blast search: – Propred I: – SVMHC: – SYFPEITHI: + NIH prediction server: + CTLPred: + Epijen: –	+
The variant peptide SH: Histidine	MHC BN Blast search: + Propred I: Not done SVMHC: – SYFPEITHI: + NIH prediction server: – CTLPred: – Epijen: –	+
The amino acids of the TCR contact site P8	Prediction results of immunoinformatics servers	Recognised by H-2K^d-restricted respiratory syncytial virus-specific CD8 T lymphocytes
The original peptide M2:82–90: Asparagine	MHC BN Blast search: + Propred I:+ SVMHC: + SYFPEITHI: + NIH prediction server: + CTLPred: + Epijen: +	+
The variant peptide NG: Glycine	MHC BN Blast Search: + Propred I:+ SVMHC: + SYFPEITHI: + NIH prediction server: + CTLPred: + Epijen: +	–

+: Identified as the epitope; –: not identified as the epitope.

tides are different from that of proteins. Several analysis criteria were modelled on various peptides from MHC–peptide and peptide–TCR interfaces of crystal templates. All H-2K^b–peptide–TCR crystal templates were collected from the protein data bank. After this, multiple structure alignment tools[49] were installed for superimposition of all peptide–H2-K^b crystal complexes to detach from TCR structures with better stereoscopic views. The results of the alignment for multiple peptide sequences as well as for crystal structures of H2-K^b bound with peptides are presented in Fig. 6(a) as three-dimensional structures of the peptide–MHC interface. Although peptides have diverse amino acid sequences (the sequence identity between 1fo0_P and 1g6r_P, 1fo0_P and 1nam_P, or 1fo0_P and 3cvh_C are 0) (Fig. 6a(1)), peptide backbones adapt an extremely conserved conformation (Fig. 6a(2)).

More accurate epitope prediction by the immunoinformatical programme integrated with the TCR contact information

We exploited our scoring function for the prediction of variant peptides, originating from the NS2:114–121 peptide of NS2 protein from influenza A/WSN/33 virus (Table 1). The template-based scoring function simulated the selected template from eight different H2-K^b–peptide–TCR crystal structures to distinguish virus-specific CD8 T-lymphocyte variant epitopes of mutant NS2 proteins

Table 3.

Amino acids of the anchor motifs P5	Prediction results of immunoinformatics servers	Recognised by H-2K^b-restricted H1N1/ WSN/33-specific CD8 T lymphocytes
The original peptide NS2:114–121: Phenylalanine	SVMHC: + SYFPEITHI: + NIH prediction server: + BIOXGEM: +	+
The variant peptide GQ: Glycine	SVMHC: − SYFPEITHI: − NIH prediction server: − BIOXGEM: −	−
The amino acids of the TCR contact site P6	**Prediction results of immunoinformatics servers**	**Recognised by H-2K^b-restricted H1N1/ WSN/33-specific CD8 T lymphocytes**
The original peptide NS2:114–121: Phenylalanine	SVMHC: + SYFPEITHI: + NIH prediction server: + BIOXGEM: +	+
The variant peptide FG: Glycine	SVMHC: + SYFPEITHI: + NIH prediction server: + BIOXGEM: −	−

+: Identified as the epitope; −: not identified as the epitope.

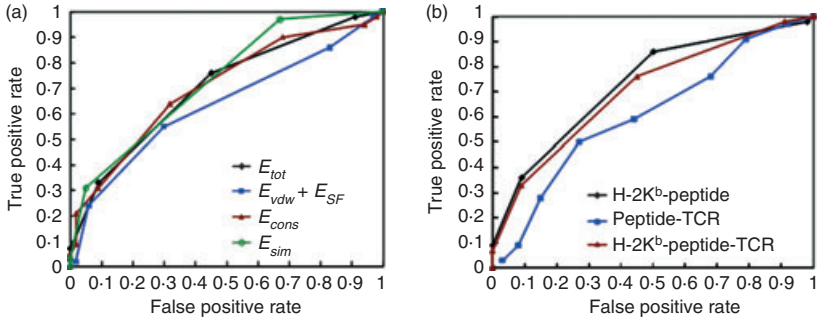

Figure 4. Evaluation of the scoring function on H2-K^b–peptide–T-cell receptor (TCR) interactions. (a) The receiver operating characteristics curve of different defined terms of scoring function. (b) Appliance of scoring function to either MHC or TCR side as well as to both interfaces.

from the original sequence. To assess the predictability of the template-based scoring function, the original and mutant sequences from the NS2 protein of H1N1 A/WSN/33 virus were inputted into the server BIOXGEM for epitope prediction. The mutant sequence of the NS2 protein with the variant peptide, designated as GQ, has the fifth anchor motif glycine (G) replacing the original phenylalanine (F) (F5→G5). Another amino acid sequence of mutant NS2 protein with the FG variant peptide encompasses the glycine (G) at the sixth TCR contact site that substitutes the original glutamine (Q) (Q6→G6). Original NS2:114–121 peptide and variant peptides, GQ and FG, are ranked as aligned amino acid sequences (Fig. 6b(1)). Anchor motif mutations only influence the rank of peptide–MHC class I binding capacity (rank 8 for NS2:114–121 and 46 for GQ) (Table 3; Figs 1 and 6b(1)). The fifth anchor motif mutation has no impact on the recognition of peptide-H-2K^b by the TCR side (rank 28 for both of NS2:114–121 and GQ) (Figs 2b and 6b(1)). In contrast to anchor motif mutation, a mutation at the sixth TCR contact site decreases the binding forces and the recognition capacity between the TCR and variant peptide FG (rank 28 for NS2:114–121 and 79 for FG), which has slight effects on the MHC side (Table 3; Figs 1b and 2b). The accuracy and precision of predictability is further improved if more than one interface is integrated into the template-based scoring function to distinguish a variety of mutant epitopes from the original (MHC&TCR sides, rank 6 for NS2:114–121, 25 for FG and 39 for GQ) (Table 1; Fig. 6b(1)).

The selected peptide–H-2K^b interface as the template from crystal structures is presented in Fig. 6b(2).[50] NS2:114–121, GQ and FG peptides are simulated with the same H-2K^b and TCR from the template crystal structure

(a)

	GLY	ALA	VAL	LEU	ILE	MET	PRO	PHE	TRP	TYR	CYS	SER	THR	ASN	GLN	HIS	ARG	LYS	ASP	GLU
GLY	0·1	−0·7	−0·8	−0·8	−0·5	−0·4	−0·4	−0·3	0·2	0·0	−0·2	−0·8	−0·3	−0·5	−0·2	−0·1	0·1	−0·4	−0·8	−1·1
ALA	−0·7	0·3	−0·3	0·1	−0·2	0·3	−0·5	0·6	0·3	0·0	−0·6	−1·1	−0·9	−0·6	−0·5	−0·2	−0·6	−1·2	−1·0	−1·0
VAL	−0·8	−0·3	1·5	1·1	0·9	1·1	−0·2	1·2	0·3	0·6	−0·3	−0·9	−0·1	−0·8	0·1	−0·4	−0·1	−0·6	−1·0	−0·5
LEU	−0·8	0·1	1·1	2·3	1·4	1·3	0·0	1·3	1·2	0·6	−0·2	−0·6	−0·2	−0·4	0·3	0·6	0·2	−0·9	−1·3	−0·3
ILE	−0·5	−0·2	0·9	1·4	2·3	1·2	0·1	1·7	1·5	1·0	−0·9	−1·2	0·1	−0·5	0·1	−0·3	−0·1	−0·8	−0·9	−0·4
MET	−0·4	0·3	1·1	1·3	1·2	3·0	0·5	1·8	1·2	1·0	0·4	−0·5	0·0	−0·4	−0·2	0·3	0·1	0·0	−1·3	0·0
PRO	−0·4	−0·5	−0·2	0·0	0·1	0·5	0·4	0·5	1·5	0·9	0·0	−0·5	−0·2	0·0	0·5	−0·3	0·0	−0·7	−0·8	−0·1
PHE	−0·3	0·6	1·2	1·3	1·7	1·8	0·5	2·7	2·1	1·2	−0·1	−0·4	0·6	0·1	0·5	0·1	0·5	−0·6	−0·9	−0·1
TRP	0·2	0·3	0·3	1·2	1·5	1·2	1·5	2·1	2·9	1·1	0·3	−0·3	0·3	0·9	0·7	0·6	0·9	0·1	0·0	−0·6
TYR	0·0	0·0	0·6	0·6	1·0	1·0	0·9	1·2	1·1	1·4	0·3	0·1	0·1	0·6	0·9	0·8	1·0	0·5	0·5	0·5
CYS	−0·2	−0·6	−0·3	−0·2	−0·9	0·4	0·0	−0·1	0·3	0·3	−0·1	−0·3	−1·1	−1·6	−1·0	0·5	−0·9	−1·3	−2·2	−1·1
SER	−0·8	−1·1	−0·9	−0·6	−1·2	−0·5	−0·5	−0·4	−0·3	0·1	−0·3	0·4	−0·5	0·0	−0·3	−0·3	−0·1	−0·3	−0·1	−0·1
THR	−0·3	−0·9	−0·1	−0·2	0·1	0·0	−0·2	0·6	0·3	0·1	−1·1	−0·5	0·6	0·0	0·0	0·1	0·1	−0·6	−0·2	−0·2
ASN	−0·5	−0·6	−0·8	−0·4	−0·5	−0·4	0·0	0·1	0·9	0·6	−1·6	0·0	0·0	1·4	0·4	−0·2	0·3	0·0	0·3	−0·2
GLN	−0·2	−0·5	0·1	0·3	0·1	−0·2	0·5	0·5	0·7	0·9	−1·0	−0·3	0·0	0·4	1·6	0·2	0·7	0·2	0·4	0·1
HIS	−0·1	−0·2	−0·4	0·6	−0·3	0·3	−0·3	0·1	0·6	0·8	0·5	−0·3	0·1	−0·2	0·2	2·1	0·3	−0·8	0·8	0·8
ARG	0·1	−0·6	−0·1	0·2	−0·1	0·1	0·0	0·5	0·9	1·0	−0·9	−0·1	0·1	0·3	0·7	0·3	1·3	−0·5	1·8	1·9
LYS	−0·4	−1·2	−0·6	−0·9	−0·8	0·0	−0·7	−0·6	0·1	0·5	−1·3	−0·3	−0·6	0·0	0·2	−0·8	−0·5	0·0	1·2	1·6
ASP	−0·8	−1·0	−1·0	−1·3	−0·9	−1·3	−0·8	−0·9	0·0	0·5	−2·2	−0·1	−0·2	0·3	0·4	0·8	1·8	1·2	0·0	−0·9
GLU	−1·1	−1·0	−0·5	−0·3	−0·4	0·0	−0·1	−0·1	−0·6	0·5	−1·1	−0·1	−0·2	−0·2	0·1	0·8	1·9	1·6	−0·9	0·7

(b)

	GLY	ALA	VAL	LEU	ILE	MET	PRO	PHE	TRP	TYR	CYS	SER	THR	ASN	GLN	HIS	ARG	LYS	ASP	GLU
GLY	0·1	−0·7	−0·8	−0·8	−0·5	−0·4	−0·4	−0·3	0·2	0·0	−0·2	−0·8	−0·3	−0·5	−0·2	−0·1	0·1	−0·4	−0·8	−1·1
ALA	−0·7	1·1	−0·6	−1·3	−1·1	−0·8	−0·7	−1·4	−1·4	−1·9	−0·5	−0·3	−0·7	−0·9	−0·9	−0·7	−1·8	−1·4	−1·1	−0·8
VAL	−0·8	0·6	0·7	−0·4	0·1	0·2	−0·2	−0·7	−1·0	−1·6	0·3	0·1	0·1	−0·8	−0·8	−0·8	−0·8	−0·8	−0·8	−0·6
LEU	−0·8	0·7	0·1	1·1	−0·1	0·5	0·0	−0·4	−0·4	−1·5	0·2	0·4	−0·1	−0·7	0·0	0·2	−0·6	−0·4	−0·5	−0·5
ILE	−0·5	0·6	0·3	0·2	0·6	0·1	−0·3	−0·7	−1·3	−0·9	−1·1	0·0	0·2	−0·4	−0·4	−0·4	−1·3	−0·7	−0·6	−0·4
MET	−0·4	1·5	1·0	0·5	0·5	1·3	0·5	0·2	0·4	0·2	0·6	0·4	0·2	−1·2	−0·3	0·3	−0·4	0·3	−0·2	0·1
PRO	−0·4	0·4	−0·8	−0·7	−1·1	0·2	0·6	−0·2	−0·6	−1·0	0·3	0·0	0·0	0·2	−0·3	−0·5	−0·4	−0·1	−0·7	−0·6
PHE	−0·3	1·5	0·3	0·7	0·6	0·9	0·9	1·0	0·8	0·1	0·2	0·5	0·6	0·2	0·3	−0·2	−0·5	0·2	−0·2	0·0
TRP	0·2	1·3	0·6	0·8	1·4	1·5	2·2	0·4	1·1	0·9	2·3	0·5	0·9	1·6	0·4	1·2	1·1	0·7	1·1	−0·5
TYR	0·0	1·2	0·3	0·0	0·2	0·7	1·1	0·7	−0·8	0·4	1·3	0·9	0·5	0·9	0·8	0·6	0·5	1·0	0·6	0·3
CYS	−0·2	0·8	−1·3	−1·0	−0·5	−1·3	−0·1	−0·4	−3·1	−1·3	1·0	1·2	−0·9	−0·6	−0·9	−1·2	−0·4	−1·4	−1·2	−1·2
SER	−0·8	0·6	−0·8	−0·6	−0·9	−0·5	0·0	−1·4	−1·8	−1·2	−0·2	0·8	0·0	−0·5	−1·8	−1·5	−1·3	−1·0	−0·1	−0·7
THR	−0·3	0·4	−0·3	−0·4	−0·4	−0·5	−0·1	−1·0	−0·8	−0·7	0·2	0·5	0·5	−0·1	−1·2	−0·9	−0·8	−0·5	0·3	−0·9
ASN	−0·5	0·9	−0·1	−0·1	−0·4	−1·0	0·2	0·1	−0·4	−0·3	0·5	0·8	0·7	1·4	−0·3	0·3	−0·3	−0·1	0·4	−0·6
GLN	−0·2	0·9	0·4	0·5	0·2	0·4	0·8	0·7	−0·1	−0·2	0·7	1·3	0·4	0·7	1·1	0·0	−0·4	−0·2	0·4	0·4
HIS	−0·1	1·2	−0·4	0·2	−0·8	−0·8	−0·3	−0·2	0·1	−0·7	0·8	0·9	0·0	0·0	−0·2	1·4	−0·4	−0·5	0·4	−0·3
ARG	0·1	1·3	0·4	0·5	0·2	0·3	1·0	0·4	0·1	−0·2	0·5	1·1	1·0	0·7	0·3	0·5	0·5	0·0	1·6	0·9
LYS	−0·4	−0·1	−0·7	−0·7	−1·3	−0·6	0·0	−0·7	−0·5	−1·1	−0·1	0·8	−0·5	0·0	0·0	−0·3	−1·7	0·3	0·3	0·6
ASP	−0·8	0·3	−1·4	−1·6	−1·0	−2·4	−0·3	−2·3	−1·5	−1·3	−0·7	0·6	0·1	−0·2	−0·4	−0·1	−0·6	−1·2	−0·1	−1·9
GLU	−1·1	0·4	−0·2	−0·5	−0·7	0·1	0·0	−0·3	−1·2	−1·2	0·2	0·7	0·1	−0·2	−0·6	−0·8	−0·3	−0·1	−0·6	−0·2

(c)

	GLY	ALA	VAL	LEU	ILE	MET	PRO	PHE	TRP	TYR	CYS	SER	THR	ASN	GLN	HIS	ARG	LYS	ASP	GLU
GLY	0	0	0	0	0	0	0	0	0	0	0	0	0	0	0	0	0	0	0	0
ALA	0	0	0	0	0	0	0	0	0	0	0	0	0	0	0	0	0	0	0	0
VAL	0	0	0	0	0	0	0	0	0	0	0	0	0	0	0	0	0	0	0	0
LEU	0	0	0	0	0	0	0	0	0	0	0	0	0	0	0	0	0	0	0	0
ILE	0	0	0	0	0	0	0	0	0	0	0	0	0	0	0	0	0	0	0	0
MET	0	0	0	0	0	0	0	0	0	0	0	0	0	0	0	0	0	0	0	0
PRO	0	0	0	0	0	0	0	0	0	0	0	0	0	0	0	0	0	0	0	0
PHE	0	0	0	0	0	0	0	0	0	0	0	0	0	0	0	0	0	0	0	0
TRP	0	0	0	0	0	0	0	0	0·0	2·2	0·0	3·2	3·7	4·4	3·1	0·0	0·0	0·0	5·1	4·5
TYR	0	0	0	0	0	0	0	0	2·2	3·7	4·0	4·4	4·0	4·7	5·0	4·7	4·6	4·2	5·5	5·5
CYS	0	0	0	0	0	0	0	0	0·0	4·0	8·0	2·4	0·0	2·6	2·8	3·9	0·0	0·0	3·2	3·1
SER	0	0	0	0	0	0	0	0	3·2	4·4	2·4	4·9	4·3	4·5	4·1	4·6	4·4	4·1	5·4	5·4
THR	0	0	0	0	0	0	0	0	3·7	4·0	0·0	4·3	4·8	4·7	4·8	3·2	4·4	4·0	5·2	4·8
ASN	0	0	0	0	0	0	0	0	4·4	4·7	2·6	4·5	4·7	5·6	4·7	4·5	4·6	4·4	5·2	4·7
GLN	0	0	0	0	0	0	0	0	3·1	5·0	2·8	4·1	4·8	4·7	5·7	4·6	4·9	4·5	4·8	4·7
HIS	0	0	0	0	0	0	0	0	0·0	4·7	3·9	4·6	3·2	4·5	4·6	5·3	4·3	1·9	5·9	6·2
ARG	0	0	0	0	0	0	0	0	0·0	4·6	0·0	4·4	4·4	4·6	4·9	4·3	0·0	0·0	6·9	7·0
LYS	0	0	0	0	0	0	0	0	0·0	4·2	0·0	4·1	4·0	4·4	4·5	1·9	0·0	0·0	6·5	6·7
ASP	0	0	0	0	0	0	0	0	5·1	5·5	3·2	5·4	5·2	5·2	4·8	5·9	6·9	6·5	0·0	0·0
GLU	0	0	0	0	0	0	0	0	4·5	5·5	3·1	5·4	4·8	4·7	4·7	6·2	7·0	6·7	0·0	0·0

(d)

	GLY	ALA	VAL	LEU	ILE	MET	PRO	PHE	TRP	TYR	CYS	SER	THR	ASN	GLN	HIS	ARG	LYS	ASP	GLU
GLY	0·0	0·0	0·0	0·0	0·0	0·0	0·0	0·0	0·0	0·0	0·0	0·0	0·0	0·0	0·0	0·0	0·0	0·0	0·0	0·0
ALA	0·0	0·0	0·0	0·0	0·0	0·0	0·0	0·0	0·0	0·0	0·0	0·0	0·0	0·0	0·0	0·0	0·0	0·0	0·0	0·0
VAL	0·0	0·0	0·0	0·0	0·0	0·0	0·0	0·0	0·0	0·0	0·0	0·0	0·0	0·0	0·0	0·0	0·0	0·0	0·0	0·0
LEU	0·0	0·0	0·0	0·0	0·0	0·0	0·0	0·0	0·0	0·0	0·0	0·0	0·0	0·0	0·0	0·0	0·0	0·0	0·0	0·0
ILE	0·0	0·0	0·0	0·0	0·0	0·0	0·0	0·0	0·0	0·0	0·0	0·0	0·0	0·0	0·0	0·0	0·0	0·0	0·0	0·0
MET	0·0	0·0	0·0	0·0	0·0	0·0	0·0	0·0	0·0	0·0	0·0	0·0	0·0	0·0	0·0	0·0	0·0	0·0	0·0	0·0
PRO	0·0	0·0	0·0	0·0	0·0	0·0	0·0	0·0	0·0	0·0	0·0	0·0	0·0	0·0	0·0	0·0	0·0	0·0	0·0	0·0
PHE	0·0	0·0	0·0	0·0	0·0	0·0	0·0	0·0	0·0	0·0	0·0	0·0	0·0	0·0	0·0	0·0	0·0	0·0	0·0	0·0
TRP	0·0	4·5	0·0	2·8	3·3	0·0	3·2	3·4	0·0	0·0	3·3	3·1	3·1	0·0	3·5	0·0	0·0	3·2	3·2	0·0
TYR	4·1	3·8	4·4	3·6	4·0	3·6	4·5	3·7	4·1	3·8	3·6	2·8	2·8	4·8	3·1	3·5	4·3	4·0	4·4	3·8
CYS	4·7	4·4	4·5	4·5	4·0	3·8	4·4	4·2	5·2	2·9	3·7	4·5	3·9	4·1	4·5	4·0	4·4	4·9	5·1	3·5
SER	4·6	4·9	3·8	4·7	4·7	4·4	3·9	2·7	4·2	2·8	4·3	5·1	4·7	3·9	2·1	0·0	3·8	4·8	3·9	4·4
THR	4·9	4·1	4·1	3·9	4·0	3·7	3·5	2·0	4·2	4·2	4·5	4·4	4·8	3·3	2·8	3·9	3·8	3·8	4·7	4·0
ASN	4·8	5·3	4·7	5·0	4·2	4·6	4·0	4·8	4·7	5·2	4·9	4·9	5·3	5·4	5·1	4·6	4·9	4·9	4·9	4·3
GLN	5·1	4·8	5·1	5·3	5·3	5·0	4·4	5·6	4·6	5·1	4·4	5·5	5·3	4·8	5·0	4·6	4·6	4·4	4·7	4·7
HIS	4·9	4·8	4·6	4·5	3·8	4·0	4·4	4·5	5·0	4·9	2·7	3·9	4·1	4·1	4·2	5·2	3·5	4·0	4·6	3·8
ARG	5·9	5·3	5·2	5·3	4·8	5·2	5·3	5·3	5·4	4·5	5·2	5·4	5·6	5·0	5·0	5·2	4·8	4·5	5·2	5·4
LYS	4·9	3·8	3·5	4·2	3·6	2·7	4·5	4·4	4·3	4·7	3·6	4·9	4·4	5·0	4·6	4·0	3·7	5·2	4·7	5·0
ASP	4·9	4·5	3·4	3·4	4·5	2·6	0·0	2·7	4·3	3·9	2·7	5·1	4·6	4·5	4·0	4·2	4·3	4·0	3·3	3·9
GLU	4·7	5·0	4·7	4·6	4·4	4·6	0·0	4·8	4·2	3·4	3·5	5·1	4·4	4·5	4·3	2·5	4·4	4·4	4·0	4·1

Figure 5. Template-based protein–protein interaction scoring matrices. (a) Side chain–side chain van der Waals scoring matrix; (b) Side chain–backbone van der Waals scoring matrix; (c) Side chain–side chain special bond scoring matrix; (d) Side chain-backbone special bond scoring matrix. The side chain–side chain scoring matrices are symmetrical, whereas side chain–backbone scoring matrices are non-symmetrical. For side chain–side chain van der Waals scoring matrix, the scores are high (yellow blocks) if large aliphatic residues (i.e. valine, leucine, isoleucine and methionine) interact with large aliphatic residues or aromatic residues (i.e. phenylalanine, tyrosine and tryptophan) interact with aromatic residue. In contrast, the scores are low (orange blocks) when non-polar residues interact with polar residues. The two highest scores are 3.0 (methionine interacting with methionine) and 2.9 (tryptophan interacting with tryptophan). For side chain–side chain special bond scoring matrix, the scores are high (pink blocks) when interacting residues (i.e. cysteine to cysteine) form disulfide bonds or basic residues (i.e. arginine, lysine and histidine) interact with acidic residues (aspartic acid and glutamic acid). The scoring values are zero if non-polar residues interact with other residues.

(Fig. 6b(3,4,5)). As the backbones of several H-2K^b-bound peptides adopt the same conformation, we have speculated on many features of the critical contact residues to be the main factors to affect specific recognition by TCR (Figs 6a(2),b). At the fifth anchor motif, substitution of phenylalanine (F) with glycine (G) could undermine the binding forces of GQ to H-2K^b because of the lack of an inward benzyl group without compromising the recognition of the outward side chain via TCR (Fig. 6b(3,4)). The substitution of glutamine (Q) with glycine (G) at the sixth TCR contact site has removed the outward amide side chain from recognition by specific TCR (Fig. 6b (3,5)). Simulation results are compatible with those obtained from laboratory experiments (Tables 2 and 3; Figs 2 and 5). The simulation approach with TCR contact information has more accurate prediction results on epitope identification than all previous computing programmes.

Discussion

Respiratory syncytial virus causes bronchiolitis and pneumonia in infants and young children.[51] Influenza A virus still represents one of the major respiratory viruses causing significant morbidity and mortality in severe respiratory tract infections.[52] In the 1960s, the trials of formalin-inactivated vaccines not only failed to protect those people who were vaccinated from RSV infection but induced deviant pathological consequences.[53] The lack of CD8 T-lymphocyte responses has been associated

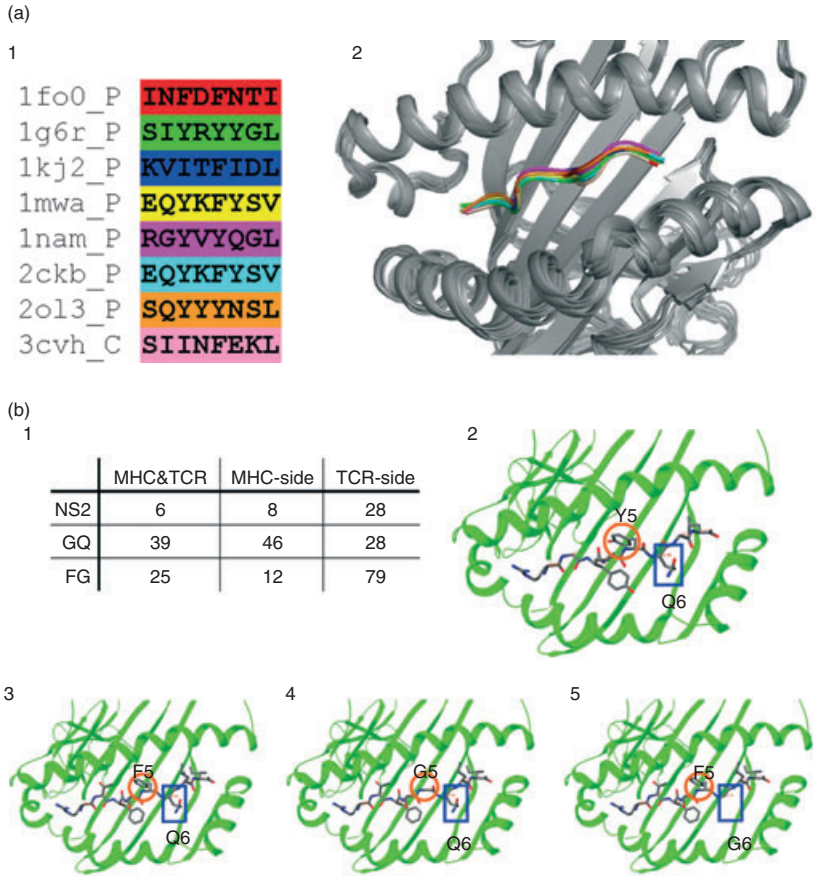

Figure 6. Structural analysis of critical binding sites on peptides in H-2K^b–peptide–T-cell receptor (TCR) crystal structures. (a) (1) Alignment of amino acid sequences from different H-2K^b-restricted epitopes and (2) Superimpose three dimensional structures of eight different H-2K^b-restricted epitopes from H2-K^b–peptide–TCR crystal complexes. (b) The scoring function is implicated in the epitope prediction on original and mutated NS2 proteins of H1N1 A/WSN/33 influenza virus: NS2:114–121, GQ and FG. (1) The rank of NS2:114–121 and peptide versions with point mutations on either MHC (GQ) or TCR side (FG). (2) The peptide–MHC interface of the selected template crystal structure (protein data bank code: 1nam). Simulated peptide–MHC interfaces of variant peptides and the original one (3) the original NS2:114–121, (4) GQ, and (5) FG (Table 1). The side chain of the fifth anchor motif (orange circle). The side chain of the sixth TCR contact site (blue rectangle).

with pulmonary eosinophilia that was observed in vaccinated people or experimental animals.[7,53,54] Antigenic drifts and heterotypic influenza A viruses continue to cause annual epidemics and pandemic outbreaks.[4,6] It is critical to identify the important elements constituting the epitope to enable CD8 T-lymphocyte recognition as well as to map mutant epitopes from mutable pathogens, either for experimental research or for immunoinformatical programmes.

The role of anchor motifs of peptides in the binding to MHC class I molecules is known and well-studied.[19–22] Immunologists and microbiologists have long relied on these anchor motifs to predict MHC class I-restricted epitopes from the protein sequences of viral pathogens. Several peptide–MHC class I binding methods have been developed to map CD8 T-lymphocyte epitopes. Consistent with the previous publication of competitive binding experiments, M2:82–90 had the highest binding affinity to H-2K^d molecules to be detected by RMA-S-K^d cells[22] (Figs 1a,c and Supplementary material, Fig. S2). Similar to M2:82–90, the substitution of the P2 anchor motif with the analogous aromatic side chain did not decrease the binding affinity of the SF peptide to H-2K^d molecules. Nevertheless, the heterologous aromatic side chains at the P2 anchor motif resulted in the reduction of the binding affinity of variant peptides to H-2K^d molecules (Fig. 1c and Supplementary material, Fig. S3). The structural similarity of side chains is required for anchor motifs to dock peptide epitopes into the pocket of MHC class I molecules. The peptide–MHC binding interface is more tolerant of the subtle change of the functional group at the anchor motif of natural amino acids, such as phenylalanine (F) replacing tyrosine (Y). The binding capacity of peptides to MHC class I molecules had become the most important consideration for the epitope prediction of immunoinformatical programmes. Most servers developed for the prediction of epitopes were based on peptide–MHC binding affinity.[27–30,32] As in much of the

documented research into peptide–MHC class I binding experiments, we have mapped CD8 T-lymphocyte variant epitopes without obvious anchor motifs of primary amino acid sequences, which were still recognised by virus-specific CD8 T lymphocytes (Fig. 1c and 2). Anchor motifs and peptide–MHC binding affinity are not sufficient to predict all the protective epitopes from viral antigens[22,45,46] (Fig. 2).

T-cell receptor binding of expressed specific peptide–MHC class I complexes on the surfaces of infected cells is less understood in the field of T-lymphocyte recognition.[26,31,55] We have found that the efficient binding of peptides to MHC class I molecules does not always ensure the recognition of peptide–MHC class I complexes by either virus-specific or peptide-specific CD8 T lymphocytes (Figs. 1, 2 and 3). Peptide–MHC class I binding and TCR recognition are actually two distinct antigen presentation events given that variant peptides with amino acid substitutions at the TCR contact site obscure the recognition of specific CD8 T lymphocytes without compromising their binding capacity to MHC class I molecules even in the presence of analogous side chains of natural amino acids (Figs 1c, 2a and 3b).

Parallel to two distinct antigen presentation events: peptide-MHC class I binding and TCR recognition, physiochemical distributions of amino acids from MHC class I-restricted epitopes represent two separated interfaces of discrete physiochemical characteristics. Conserved and hydrophobic amino acids are identified at P2 and P9 anchor motifs on the peptide-H-2K^{d} interface (Supplementary material, Fig. S4a), whereas the peptide–TCR interface expresses variable amino acid distributions in terms of hydropathy and isoelectric indexes (Supplementary material, Fig. S4). Extensive data from X-ray diffraction crystal structures of different alleles of MHC–peptide–TCR complexes provides detailed binding and recognition information of interfaces among peptide, MHC and TCR.[56–64] The TCR recognition of contact amino acids from peptides presented by MHC molecules depends on the complementarity determining regions of variable domains.[50,56–65] The conserved conformation of main chain from H-2K^{b}-bound peptides has been observed in several crystal structures without similarity of amino acid sequences[62,63] (Fig. 6a). These observations indicate the importance of the side chain structures of natural amino acids in TCR recognition of variant peptides with point mutations at anchor motifs or TCR contact sites[62,63,65,66] (Fig. 6b; Tables 2 and 3). Inconsistent with the observation that the peptide–MHC side is more tolerant to subtle changes at the side chain, the TCR distinguishes various side chains at the peptide–TCR interface (Table 1; Figs 1c and 2a). Notwithstanding the significance of analogous side chains at TCR contact sites, the variant peptide consisting of natural amino acids inhibits the recognition of specific TCR with the analogous functional group indicating that the TCR has recognised the steric structure of the functional group instead of side chain conformations at the TCR contact site[65,66] (Fig. 2a).

Although the interaction of peptide and TCR has been modelled with simulation, similarity and software analysis for each TCR contact residue of epitopes, the interface between peptides and TCR is still far behind the expectation for accurate and precise epitope prediction.[31,55] The lack of solid data on the interaction between peptide and TCR, and hence the lack of appropriate prediction criteria, hinders the progress of prediction from better immunoinformatical programmes. We have developed an amino acid substitution approach to elucidate the impact of single amino acid substitutions of the TCR contact site on the prediction accuracy of immunoinformatical programmes (Table 1; Figs 1, 2 and 3). None of the programmes that this research employed predicted the epitopes of variant peptides with accuracy and precision except BIOXGEM, which is integrated with the interaction information of the peptide–TCR contact interface, which offered consistent prediction results compared with those from laboratory experiments. (Tables 2 and 3; Figs 2 and 3). The importance of the TCR contact site has been demonstrated in three experimental systems, photoaffinity labelling of the peptide, peptide–MHC class I binding experiments and functional recognition assays of variant peptides by specific CD8 T lymphocytes, in three different pathogens, *Plasmodium*,[26] RSV and influenza A/WSN/33 virus (Figs 1, 2 and 3). The binding of peptides to MHC class I molecules should no longer be the only essential criterion for epitope prediction. TCR contact residues are as essential as anchor motifs for recognition by CD8 T lymphocytes. The TCR contact residue is another imperative domain to be integrated into immunoinformatical programmes for epitope prediction. More structural research on the different alleles of peptide–MHC–TCR complexes will further expand the capacity of simulation programmes to predict protective epitopes from other mutable viruses.

Escape mutants of RSV to protective monoclonal antibody for prophylactic treatment have been isolated from a murine model that is semi-permissive to RSV replication.[67] The antigenic drift of nucleoprotein from influenza A virus has been spotted at anchor motifs of CD8 T-lymphocyte epitopes.[68,69] Besides, the effect of antigenic drift on non-anchor regions of epitopes escapes recognition by specific CD8 T lymphocytes.[70] Most mutation sites of mutant CD8 T-lymphocyte epitopes have been recently located at non-anchor residues or TCR contact regions from frequently mutable viruses, such as HIV.[71] Very few mutation hotspots have been found at anchor motifs. Data from Figs 1, 2 and 3 suggest that mutations at TCR contact residues are more likely for the mutant virus to retain the ability of mutant epitopes to bind to MHC class I molecules as well as to reduce CD8 T-lym-

phocyte-mediated immune responses against pathogens. Data in Figs 2 and 3 show that *in vitro* re-stimulation with variant peptides does not enhance any immune responses primed by the original immunodominant CD8 T-lymphocyte epitope of the RSV infection, which conflicts with 'original antigenic sin', in which subsequent mutant virus infection often enhances immune responses to original epitopes rather than mutant epitopes *in vivo*.[72]

The cocktail multi-epitope vaccine is a promising approach to elicit protective immunity while bypassing pathogenic regions of RSV antigens.[13,73,74] To stimulate both humoral and cellular immune responses with cocktail multi-epitope vaccines enables the prevention of escape mutant viruses, like zoonotic influenza viruses.[13,15,17,75] Variant peptides are important not only for the epitope prediction of mutable viruses but also for the design of cocktail multi-epitope vaccines to prevent viral infections that are difficult to block with conventional vaccines.

Acknowledgements

The work is supported by Intramural Research Funding for Dr Shiou-Chih Hsu by the Vaccine Research and Development Centre, National Health Research Institute, Taiwan from 2005 to 2007, project number: VC-095-PP-05. Part of the work is supported by National Science Council projects funded for Professor Jinn-Moon Yang by the National Science Council project number: 98-2627-B-009-003 and 98-3112-B-009-003, Department of Biological Science and Technology, Institute of Bioinformatics and Systems Biology, Hsinchu City, Taiwan. We would like to thank the programmers and others who made available the epitope prediction servers and websites. Their work has helped to improve this research; and we hope that this research will help to improve such services.

Website addresses for epitope prediction servers

http://www-bimas.cit.nih.gov/molbio/hla_bind/
http://www.darrenflower.info/EpiJen/
http://www.imtech.res.in/raghava/propred1/
http://www.imtech.res.in/raghava/ctlpred/
http://www.syfpeithi.de/Scripts/MHCServer.dll/EpitopePrediction.htm
http://www-bs.informatik.uni-tuebingen.de/Services/SVMHC
http://140.113.239.233/~hiwind/MHC_peptide_TCR/index.php

We would like to thank for Dr Johnathan W. Yewdell, Dr Jack Bennink and Dr John E. Coligan for providing RMA, RMA-S and RMA-S-K^d cells for peptide–MHC class I binding experiments.

References

1 Isaacs D, Bangham CRM, McMichael AJ. Cell-mediated cytotoxic responses to respiratory syncytial virus in infants with bronchiolitis. *Lancet* 1987; **2**:769–71.
2 Isaac D, Taylor CJ, Ting A, McMichael AJ. HLA class I antigens in severe RSV bronchiolitis. *Tissue Antigens* 1989; **34**:210–2.
3 Mbawuike IN, Wells J, Byrd R, Cron SG, Glezen WP, Piedra PA. HLA-restricted $CD8^+$ cytotoxic T lymphocyte, interferon-γ, and interleukin-4 responses to respiratory syncytial virus infection in infants and children. *J Infect Dis* 2001; **183**:687–96.
4 McMichael AJ, Gotch FM, Noble GR, Beare PA. Cytotoxic T-cell immunity to influenza. *N Engl J Med* 1983; **309**:13–7.
5 Stevenson PG, Hawke S, Bangham CRM. Protection against lethal influenza virus encephalitis by intranasally primed $CD8^+$ memory T cells. *J Immunol* 1996; **157**:3065–73.
6 Grebe KM, Yewdell JW, Bennink JR. Heterotypic immunity to influenza A virus: where do we stand? *Microbes and Infect* 2008; **10**:1024–9.
7 Tripp RA, Anderson LJ. Cytotoxic T-lymphocyte precursor frequencies in BALB/C mice after acute respiratory syncytial virus (RSV) infection or immunisation with a formalin-inactivated RSV vaccine. *J Virol* 1998; **72**:8971–5.
8 Hsu SC, Chargelegue D, Steward MW. Reduction of respiratory syncytial virus titer in the lung of mice after intranasal immunisation with a chimeric peptide consisting of a single CTL epitope linked to a fusion peptide. *Virology* 1998; **240**:376–81.
9 Prince GA, Mond JJ, Porter DD, Yim KC, Lan SJ, Klinman DM. Immunoprotective activity and safety of a respiratory syncytial virus vaccine: mucosal delivery of fusion glycoprotein with a CpG oligodeoxynucleotide adjuvant. *J Virol* 2003; **77**:13156–60.
10 Carbone FR, Bevan MJ. Class I-restricted processing and presentation of exogenous cell-associated antigen *in vivo*. *J Exp Med* 1990; **171**:377–87.
11 Schirmbeck R, Melber K, Mertens T, Reimann J. Antibody and cytotoxic T-cell responses to soluble hepatitis B virus (HBV) S antigen in mice: implication for the pathogenesis of HBV-induced hepatitis. *J Virol* 1994; **68**:1418–25.
12 Kast WM, Roux L, Curren J, Blom HJ, Voordouw AC, Meloen RH, Kolakofsky D, Melief CJM. Protection against lethal Sendai virus infection by *in vivo* priming of virus specific cytotoxic T lymphocytes with a free synthetic peptide. *Proc Natl Acad Sci USA* 1991; **88**:2283–7.
13 Hsu SC, Chargelegue D, Obeid OE, Steward MW. Synergistic effect of immunisation with a peptide cocktail inducing antibody, helper and cytotoxic T-cell responses on protection against respiratory syncytial virus. *J Gen Virol* 1999; **80**:1401–5.
14 Oukka M, Manuguerra JC, Livaditis N, Tourdol S, Riche N, Vergnon I, Cordopatis P, Kosmatopoulos K. Protection against lethal viral infection by vaccination with nonimmunodominant peptides. *J Immunol* 1996; **157**:3039–45.
15 Stoloff GA, Caparros-Wanderley W. Synthetic multiepitope peptides identified *in silico* induce protective immunity against multiple influenza serotypes. *Eur J Immunol* 2007; **37**:2441–9.
16 Vitiello A, Yuan L, Chesnut RW *et al.* Immunodominance analysis of CTL responses to influenza PR8 virus reveals two new dominant and subdominant K^b-restricted epitopes. *J Immunol* 1996; **157**:5555–62.
17 Kalergis AM, Ono T, Wang F, Dilorenzo TP, Honda S, Nathenson SG. Single amino acid replacements in an antigenic peptide are sufficient to alter the TCR Vβ repertoire of the responding $CD8^+$ cytotoxic lymphocyte population. *J Immunol* 1999; **162**:7263–70.
18 Townsend A, Bodmer H. Antigen recognition by class I-restricted T lymphocytes. *Annu Rev Immunol* 1989; **7**:601–24.
19 Rammensee HG, Falk K, Rőtzschke O. Peptides naturally presented by MHC class I molecules. *Annu Rev Immunol* 1993; **11**:213–44.
20 Engelhard VH. Structure of peptides associated with class I and class II MHC molecules. *Annu Rev Immunol* 1994; **12**:181–207.
21 Maryanski JL, Lűthy R, Romero P *et al.* The interaction of antigenic peptides with the H-$2K^d$ MHC class I molecule. *Semin Immunol* 1993; **5**:95–104.
22 Quesnel A, Hsu SC, Delmas A, Steward MW, Trudelle Y, Abastado JP. Efficient binding to the MHC class I K^d molecule of synthetic peptides in which the anchoring position 2 does not fit the consensus motif. *FEBS Lett* 1996; **387**:42–6.
23 Guichard G, Calbo S, Muller S, Kourilsky P, Briand JP, Abastado JP. Efficient binding of reduced peptide bond pseudopeptides to major histocompatibility complex class I molecule. *J Biol Chem* 1995; **270**:26057–9.
24 Silver ML, Guo H-C, Strominger JL, Wiley DC. Atomic structure of a human MHC molecule presenting an influenza virus peptide. *Nature* 1992; **360**:367–9.
25 Zhang W, Young AC, Imarai M, Nathenson SG, Sacchettinni JC. Crystal structure of the major histocompatibility complex class I H-$2K^b$ molecule containing a single viral peptide: implications for peptide binding and T-cell receptor recognition. *Proc Natl Acad Sci USA* 1992; **89**:8403–7.
26 Romero P, Casanova JL, Cerottini JC, Maryanski JL, Luescher IF. Differential T cell receptor photoaffinity labeling among H-$2K^d$-restricted cytotoxic T lymphocyte clones

specific for a photoreactive peptide derivative. Labelling of the α-chain correlates with Jα Segment Usage. *J Exp Med* 1993; **177**:1247–56.
27 Wan J, Liu W, Xu Q, Ren Y, Flower DR, Li T. SVRMHC prediction server for MHC-binding peptides. *BMC Bioinformatics* 2006; **7**:463.
28 Doytchinova IA, Guan P, Flower DR. EpiJen: a server for multistep T cell epitope prediction. *BMC informatics* 2006; **7**:131.
29 Larsen MV, Lundegaard C, Lamberth K, Buus S, Brunak S, Lund O, Nielsen M. An integrative approach to CTL epitope prediction: a combined algorithm integrating MHC class I binding, TAP transport efficiency and proteasomal cleavage predictions. *Eur J Immunol* 2005; **35**:2295–303.
30 Doytchinova IA, Flower DR. Predicting class I major histocompatibility complex (MHC) binders using multivariate statistics: comparison of discriminant analysis and multiple linear regression. *J Chem Inf Model* 2007; **47**:234–8.
31 Doytchinova IA, Flower DR. Modeling the peptide-T cell receptor interaction by the comparative molecular similarity indices analysis – soft independent modeling of class analogy technique. *J Med Chem* 2006; **49**:2193–9.
32 Jojic N, Reyes-Gomez M, Heckerman D, Kadie C, Schueler-Furman O. Learning MHC 1-peptide binding. *Bioinformatics* 2006; **22**:e227.
33 Rammensee H, Bachmann J, Emmerich NP, Bachor OA, Stevanovic S. SYFPEITHI: database for MHC ligands and peptide motifs. *Immunogenetics* 1999; **50**:213–9.
34 Singh H, Raghava GPS. ProPred I: prediction of promiscuous MHC class-I binding sites. *Bioinformatics* 2003; **19**:1009–14.
35 Altuvia Y, Sette A, Sidney J, Southwood S, Marglit H. A structure-based algorithm to predict potential binding peptides to MHC molecules with hydrophobic binding pockets. *Hum Immunol* 1997; **58**:1–11.
36 Chen YC, Lo YS, Hsu WC, Yang JM. 3D-partner: a web server to infer interacting partners and binding models. *Nucleic Acids Res* 2007; **35**:W561–7.
37 Townsend A, Ohlën C, Foster L, Bastin J, Ljunggren HG, Kärre K. Mutant cell in which association of class I heavy and light chains is induced by viral peptides. *Cold Spring Harb Symp Quant Biol* 1989; **1**:299–308.
38 Chen W, Yewdell JW, Levine RL, Bennink JR. Modification of cysteine residues *in vitro* and *in vivo* affects the immunogenicity and antigenicity of major histocompatibility complex class I-restricted viral determinants. *J Exp Med* 1999; **189**:1757–64.
39 Smith W, Andrewes CH, Laidlaw PP. A virus obtained from influenza patients. *Lancet* 1933; **1**:66–8.
40 Kos FJ, Müllbacher A. Enhancement of antigen-specific activation of $CD8^+$ memory cytotoxic T cells by B cell-derived factors. *Immunobiology* 1992; **186**:410–20.
41 Kos FJ, Müllbacher A. Specific epitope-induced conversion of $CD8^+$ memory cells into effector cytotoxic T lymphocytes *in vitro*: presentation of peptide antigens by $CD8^+$ T cells. *Eur J Immunol* 1992; **22**:1595–601.
42 Lo YS, Lin CY, Yang JM. PC family: a web server for searching homologous protein complexes. *Nucleic Acids Res* 2010; **38**:W516–22.
43 Kulkarni AB, Morse HC III, Bennink JR, Yewdell JW, Murphy BR. Immunisation of mice with vaccinia virus-M2 recombinant induces epitope-specific and cross-reactive K^d-restricted $CD8^+$ cytotoxic T cells. *J Virol* 1993; **67**:4086–92.
44 DiBrino M, Tsuchida T, Turner RV, Parker KC, Coligan JE, Biddison WE. HLA-A1 and HLA-A3 T cell epitopes derived from influenza virus proteins predicted from peptide binding motifs. *J Immunol* 1993; **151**:5930–5.
45 Sadovnikova E, Zhu X, Collins SM, Zhou J, Vousden K, Crawford L, Beverley P, Stauss HJ. Limitation of predictive motifs revealed by cytotoxic T lymphocyte epitope mapping of the human papillomavirus E7 protein. *Int Immunol* 1994; **6**:289–96.
46 Jiang S, Borthwick NJ, Morrison P, Gao GF, Steward MW. Virus-specific CTL responses induced by an H-$2K^d$-restricted motif-negative 15-mer peptide from the fusion protein of respiratory syncytial virus. *J Gen Virol* 2002; **83**:429–38.
47 Holtappels R, Simon CO, Munks MW *et al.* Subdominant CD8 T cell epitopes account for protection against cytomegalovirus independent of immunodomination. *J Virol* 2008; **82**:5781–96.
48 Van der Most RG, Sette A, Oseroff C *et al.* Analysis of cytotoxic T cell responses to dominant and subdominant epitopes during acute and chronic lymphocytic choriomeningitis virus infection. *J Immunol* 1996; **157**:5543–54.
49 Guda C, Lu S, Scheeff ED, Bourne PE, Shindyalov LN. CE-MC: a multiple protein structure alignment server. *Nucleic Acids Res* 2004; **32**:W100–3.
50 Reiser J-B, Darnault C, Grégoire C *et al.* CDR3 loop flexibility contributes to the degeneracy of TCR recognition. *Nat Immunol* 2003; **4**:241–7.
51 Hall CB, Weinberg GA, Iwane MK *et al.* The burden of respiratory syncytial virus infection in young children. *N Engl J Med* 2009; **360**:588–74.
52 Chowell G, Bertozzi SM, Colchero MA, Gatell HL, Alpuche-Aranda C, Hernandez M. Severe respiratory disease concurrent with the circulation of H1N1 influenza. *N Engl J Med* 2009; **361**:674–9.
53 Fulginiti VA, Eller JJ, Sieber OF, Joyner JW, Minamitani M, Meiklejohn G. Respiratory virus immunisation. A field trial of two inactivated respiratory virus vaccines; an aqueous trivalent parainfluenza virus vaccine and an alum-precipitated respiratory syncytial virus vaccine. *Am J Epidemiol* 1969; **89**:435–48.
54 Srikiatkhachorn A, Braciale TJ. Virus-specific $CD8^+$ T lymphcoytes downregulate T helper cell type 2 cytokine seretion and pulmonary eosinophilia during experimental murine respiratory syncytial virus infection. *J Exp Med* 1997; **186**:421–32.
55 Rudolph MG, Stanfield RL, Wilson IA. How TCRs bind MHCs, peptides, and coreceptors. *Annu Rev Immunol* 2006; **24**:419–66.
56 Reiser J-B, Darnault C, Guimezanes A *et al.* Crystal structure of a T cell receptor bound to an allogeneic MHC molecule. *Nat Immunol* 2000; **1**:291–7.
57 Reiser J-B, Grégoire C, Darnault C *et al.* T cell receptor CDR3β loop undergoes conformational changes of unprecedented magnitude upon binding to a peptide/MHC class I complex. *Immunity* 2002; **16**:345–54.
58 Ker-Nielsen L, Clements CS, Purcell AW, Brooks AG, Whisstock JC, Burrows SR, McCluskey J, Rossjohn J. A structural basis for the selection of dominant $\alpha\beta$ T cell receptors in antiviral immunity. *Immunity* 2003; **18**:53–64.
59 Tynan FE, Burrows SR, Buckle AM *et al.* T cell receptor recognition of a 'super-bulged' major histocompatibility complex class I-bound peptide. *Nat Immunol* 2005; **6**:1114–22.
60 Garcia KC, Degano M, Stanfield RL, Brunmark A, Jackson MR, Peterson PA, Teyton L, Wilson IA. An $\alpha\beta$ T cell receptor structure at 2.5 Å and its orientation in the TCR-MHC complex. *Science* 1996; **274**:209–19.
61 Stewart-Jones GBE, McMichael AJ, Bell JI, Stuart DI, Jones Y. A structural basis for immunodominant human T cell receptor recognition. *Nat Immunol* 2003; **4**:657–63.
62 Lee JK, Stewart-Jones G, Dong T *et al.* T cell cross-reactivity and conformational changes during TCR engagement. *J Exp Med* 2004; **200**:1455–86.
63 Theodossis A, Guillonneau C, Welland A *et al.* Constraints within major histocompatibility complex class I restricted peptides: presentation and consequences for T cell recognition. *Proc Natl Acad Sci USA* 2010; **107**:5534–9.
64 Ding Y-H, Baker BM, Garboczi DN, Biddison WE, Wiley DC. Four A6-TCR/peptide/HLA-A2 structures that generate very different T cell signals are nearly identical. *Immunity* 1999; **11**:45–56.
65 Baker MB, Gagnon SJ, Biddison WE, Wiley DC. Conversion of a T cell antagonist into agonist by repairing a defect in the TCR/peptide/MHC interface: implications for TCR signaling. *Immunity* 2000; **13**:475–84.
66 Yang JM, Tsai CH, Hwang MJ, Tsai HK, Hwang JK, Kao CY. GEM: a Gaussian evolutionary method for predicting protein side-chain conformations. *Protein Sci* 2002; **11**:1897–907.
67 Zhao X, Sullender WM. *In vivo* selection of respiratory syncytial virus resistant to palivizumab. *J Virol* 2005; **79**:3962–8.
68 Voeten JTM, Bestebroer TM, Nieuwkoop NJ, Fouchier RAM, Osterhaus ADME, Rimmelzwaan GF. Antigenic drift in the influenza A virus (H3N2) nucleoprotein and escape from recognition by cytotoxic T lymphocytes. *J Virol* 2000; **74**:6800–7.
69 Berkhoff EGM, de Wit E, Geelhoed-Mieras MM, Boon ACM, Symons J, Fouchier RAM, Osterhaus ADME, Rimmelzwaan GF. Functional constraints of influenza A virus epitopes limit escape from cytotoxic T lymphocytes. *J Virol* 2005; **79**:11239–46.
70 Boon ACM, de Mutsert G, Graus YMF, Fouchier RAM, Sintnicolaas K, Osterhaus ADME, Rimmelzwaan GF. Sequence variation in a newly identified HLA-B35-restricted epitope in the influenza A virus nucleoprotein associated with escape from cytotoxic T lymphocytes. *J Virol* 2002; **76**:2567–72.
71 Uhlin M, Masucci M, Levitsky V. Is the activity of partially agonistic MHC: peptide ligands dependent on the quality of immunological help? *Scan J Immunol* 2006; **64**:581–7.
72 Klenerman P, Zinkernagel RM. Original antigenic sin impairs cytotoxic T lymphocyte responses to viruses bearing variant epitopes. *Nature* 1998; **394**:482–5.
73 Anderson R, Huang Y, Langley JM. Prospects for defined epitope vaccines for respiratory syncytial virus. *Future Med* 2010; **4**:585–602.
74 Sparer TE, Matthews S, Hussell T, Rae AJ, Garcia-Barreno B, Melero JA, Openshaw PJM. Eliminating a region of respiratory syncytial virus attachment protein allows induction of protective immunity without vaccine-enhanced lung eosinophilia. *J Exp Med* 1998; **187**:1921–6.
75 Plotkin SA. Immunologic correlates of protection induced by vaccination. *Pediatr Infect Dis J* 2001; **20**:63–75.

Supporting Information

Additional Supporting Information may be found in the online version of this article.

Please note: Wiley-Blackwell are not responsible for the content or functionality of any supporting materials supplied by the authors. Any queries (other than about missing material) should be directed to the corresponding author for the article.